Aerosol Optical Thickness at Tabuk City, SA

Khadeejeh M. Hamasha[a+b], Hala M. Abu Mostafa[a+c], Lalitha T. Alexander [a]

[a]Department of Physics, Tabuk University, Tabuk, Saudi Arabia
[b]Department of Physics, Yarmouk University, Irbid, Jordan.
[c]Deartment of Physics, Menofia University, Menofia, Egypt.

Abstract

There is a need to recognize air pollution levels by particles, especially in the countries where data are scarce due to the absence of routine monitoring of ambient air quality. This study aims at studying the air quality in the city of Tabuk through the measurement and analysis of the aerosol optical thickness (AOT) for three different wavelength (870nm, 550nm, and 660nm).AOT were measured using sun photometer at 870nm wavelength and calculated from satellite maps at 550nm and 660nm.this measurements were conducted during July 2012. The calculations of the angstrom parameter α using the data of AOT at 550nm wavelength for each day show values ranging between 2.21 and 6.39 which indicate that the atmosphere of Tabuk city has air pollutants in the range of fine particles. The average visibility attributed to aerosol at the City Center site dominated by urban scale and regional scale was ranging from 11km to 53km.

Keywords: aerosol optical thickness, visibility, Tabuk city, sun photometer, air pollution.

Introduction

Aerosol optical Thickness (AOT) is a quantitative measure of the extinction of solar radiation by aerosol scattering and absorption between the point of observation and the top of the atmosphere. It is a measure of the integrated columnar aerosol load and the single most important parameter for evaluating direct radiative forcing. Extinction coefficient is the fractional depletion of radiance per unit path length (also called attenuation especially in reference to radar frequencies). The optical thickness along the vertical direction is also called normal optical thickness (compared to optical thickness along slant path length). AOT is a measure of aerosol loading in the atmosphere. A higher AOT value indicates higher column of aerosol loading and hence lower visibility (Wang and Christopher, 2003).

In this study AOT was calculated depending on hand hold sun photometer measurements in Tabuk city, Saudi Arabia at wavelength of 870nm.the study was held in the period of 6 July to 17 July, 2012. MODIS satellite maps were used to determine the value of AOT for the same site at the same period with two more wavelengths, 550 nm and 660 nm, and visibility calculations at wavelength 550 nm were done.

Tabuk City

Tabuk is situated in north-western Saudi Arabia. It is the northern gateway to the Kingdom, close to the Jordanian border. It is the largest city in North Western Saudi Arabia and is mainly a military town. It is spread over an area of 104,000 square kilometers. Tabuk is 2,200 feet above sea level. Standing high above sea level, the town of Tabuk enjoys an equitable climate. The climate in this area is mild in the summer when the average temperature reaches 29 degrees Celsius. During winter the average is 17 degrees Celsius although it can sometimes fall below zero. There is little rain in the area with an annual average of only 50 mm. Western, northwestern, and southwestern winds blow all year round.

Sun photometer

A sun photometer is an electronic device that measures direct sunlight over a narrow range of wavelength. That is, it measures light of a particular color. The detector used to measure sunlight determines these wavelengths.

Sun photometer was developed by Daved Brooks and Forrest Mims (Brook et. al. 1998) that used light emitting diodes (LEDs) as detectors. When sunlight strikes one of the LEDs, it produces a very small current. This signal is amplified by the electronics, which are located to the right of the detectors. Amplifiers that produce an output voltage proportional to an input current are called trans-impedance amplifiers. This device uses a double operational amplifier (op amp). The output voltage is also affected by the concentration of particles (aerosols) in the atmosphere. These particles, which are suspended in the atmosphere, scatter or absorb sunlight. The higher the concentration of aerosols, the smaller the amount of sunlight reaching the detector, and the smaller the sun photometer output voltage. So one can use the sun photometer for studying the atmosphere, and in particular for determining the atmospheric optical thickness.

MODIS

MODIS, Moderate Resolution Imaging Spectroradiometer, is a key instrument aboard the Terra (EOS AM) and Aqua (EOS PM) satellites. Terra's orbit around the Earth is timed so that it passes from north to south across the equator in the morning, while Aqua passes south to north over the equator in the afternoon. Terra MODIS and Aqua MODIS are viewing the entire Earth's surface every 1 to 2 days, acquiring data in 36 spectral bands, or groups of wavelengths

The MODIS instrument is operating on both the Terra and Aqua spacecraft. It has a viewing swath width of 2,330 km and views the entire surface of the Earth every one to two days. Its detectors measure 36 spectral bands between 0.405 and 14.385 µm, and it acquires data at three spatial resolutions -- 250m, 500m, and 1,000m.
Along with all the data from other instruments on board the Terra spacecraft and Aqua Spacecraft, MODIS data are transferred to ground stations in White Sands, New Mexico, via the Tracking and Data Relay Satellite System (TDRSS). The data are then sent to the EOS Data and Operations System (EDOS) at the Goddard Space Flight Center. The Level 1A, Level 1B, geolocation and cloud mask products and the Higher-level MODIS land and atmosphere products are produced by the MODIS Adaptive Processing System (MODAPS), and then are parceled out among three DAACs for distribution. Ocean color products are produced by the Ocean Color Data Processing System (OCDPS) and distributed to the science and applications community.

The many data products derived from MODIS observations describe features of the land, oceans and the atmosphere that can be used for studies of processes and trends on local to global scales. As just noted, MODIS products are available from several sources. MODIS Level 1 and atmosphere products are available through the LAADS web. Land Products are available through the Land Processes DAAC at the U. S. Geological Survey EROS Data Center (EDC). Cryosphere data products (snow and sea ice cover) are available from the National Snow and Ice Data Center (NSIDC) in Boulder, Colorado. Ocean color products and sea surface temperature products along with information about these products are obtainable at the OCDPS at GSFC. Users with an appropriate x-band receiving system may capture regional data directly from the spacecraft using the MODIS Direct Broadcast signal.

The MODIS AOT dataset collection was used for this study. The MODIS dark-target aerosol retrieval algorithms (Remer et al., 2008, 2009) derive aerosol properties over dark land (Levy et al., 2007).

Aerosol Optical Thickness

Aerosol optical thickness (AOT) is a number which expresses how difficult it is for light to pass through the atmosphere. A small number would mean that light could pass through the atmosphere fairly easily. A higher number would mean light is being blocked or scattered by a large amount of clouds, aerosols, and gases, and is having difficulty passing through the atmosphere.

If we want to know specifically how difficult it is for the light to pass the atmosphere, let the intensity I of a narrow beam of sunlight of a particular wavelength that reaches earth's is given by

$$I = I_0 e^{-(AOT)\,M} \qquad (1)$$

Where I_0 is the intensity of the sunlight just above Earth's atmosphere, AOT is the total atmospheric optical thickness, and M is the relative air mass. M is equal to unity when the sun is directly overhead and is otherwise approximately equal to sec (z), where z is the solar zenith angle.

The total atmospheric optical thickness can be divided into two parts, one part due to the fact that molecules in the atmosphere scatter sunlight out of a direct beam from the sun (Rayleigh scattering) and another part due to scattering by aerosols (a_a). The Rayleigh scattering term a_R is proportional to the ratio of atmospheric pressure at the observer's location to sea level atmospheric pressure, p/p_0. Hence,

$$a = a_a + a_R(p/p_0) \quad (2)$$

If a sun photometer measures light intensity such that the voltage signal produced by the instrument is directly proportional to intensity, then

$$V = V_0 (r_0/r)^2 \exp(-[a_a + a_R(p/p_0)]M) \quad (3)$$

Where V is the voltage that is recorded when a sun photometer is pointed at the sun, minus the dark voltage. r_0/r is the ratio of one astronomical unit (AU)to the actual distance from the earth to the sun, in unit of AU, at the time the measurement is taken. And V_0 is an extraterrestrial constant voltage, which is the voltage that a sun photometer would see if it is pointed at the sun just outside the earth's atmosphere when the earth is 1 AU from the sun.

Solving equation 3 for a_a,

$$a_a = [\ln(V_0 (r_0/r)^2) - \ln(V) - a_R(p/p_0)M]/M \quad (4)$$

The Rayleigh scattering term a_R depends on the wavelength at which a particular sun photometer responds to sunlight. It is a simplification to say that total atmospheric optical thickness depend just on molecular (Rayleigh) scattering and aerosols. The simplification is useful because it conceptually separates to the contributions of the natural atmosphere from contaminants such as aerosol.

Equation 4 could be written as

$$\text{AOT} = \frac{ETconstant\ -Ln(V_s - V_d)-(0.117M)(\frac{P}{1013.25})}{M} \quad (5)$$

Where: AOT ≡ Aerosol optical thickness
ET constant ≡ Extraterrestrial constant for the instrument
V_s ≡ Sun signal in volts
V_d ≡ Dark signal in volts
M ≡ Air mass
P ≡ Barometric Pressure

Because the sun photometer is aimed directly at the sun, any aerosols and gases (haze) between the sun and photometer will tend to decrease the sun's intensity as it is detected by the photodiode inside the case of the instrument. A hazy sky would result in a lower intensity and a lower voltage reading. A very clear blue sky would result in a greater intensity and a higher voltage reading.

Angstrom components

The size distribution of aerosol can be estimated from spectral aerosol optical depth, typically from 440 nm to 870 nm. The angstrom parameter, α, can calculated from two or more wavelengths using least squares fit to the line

$$\text{Ln (AOT)} = \beta - \alpha \text{ Ln}(\lambda) \quad (6)$$

β is the intercept and is not used. Values of α greater than 2.0 indicate fine mode of particles exist, while values of α near zero indicate the presence of coarse mode particles (Eck 1999).

Visibility

Visibility is defined as the maximum distance that an object or details of a complex pattern can be seen (Retail et al., 2010). The visibility can be calculated from an inversion of Vermote et al. (Vermote et al., 2002)

$$V = 3.9449/ (AOT_{550} - 0.08498) \quad (7)$$

Where V, is the visibility in kilometers since the constant 3.9449 is in km, and AOT_{550} is the aerosol optical thickness at 550 nm wavelength.

Data and Methodology

The handheld sun photometer measures the attenuation of the direct sunlight as it passes through the atmosphere. The sun photometer is a device for measuring the amount of direct sunlight. Voltmeter used with the sun photometer to record the sun intensity. With the hand holding and pressing the on button, the sun photometer was directed towards the sun while the voltmeter was held in the other hand to observe the sun intensity reading.

The value of the maximum sun signal at each measurement time was recorded as well as the dark value. The dark value is the voltmeter reading when the LED aperture is blocked and no sunlight enters the LED.

The measurements presented in this study were recorded at an urban site, the center of Tabuk city, Saudi Arabia (28.3991^{o}N, 36.5718^{o}E). The readings at 870nm were used in this study, taken every 30 min covering the period of 6 July to 17 July, 2012. MODIS satellite maps were used to determine the value of AOT for the same site at the same period with two more wavelengths, 550 nm and 660 nm. Then visibility was calculated by equation 7 at 550nm wavelength.

Results and discussions

In this study a measurements of AOT at wavelength of 870 nm using handheld sun-photometer was held in Tabuk city during the period of 6 – 17 July, 2012. Figures 2 – 13 show the correlation between the natural logarithms of the voltage recorded using the handheld sun-photometer and air mass. Values of AOT are between 0.047 and 0.065. values of AOT at the wavelength of 550 nm and 660 nm are recorded using the MODIS satellite maps, as shown in figures 14 - 36.Table 1 show the values of AOT for three wavelength for the period 6 – 17 July 2012. For each day a linear regression were done between the natural logarithm of AOT and the natural logarithm of the wavelength. From these regressions the angstrom exponents α and β were calculated and recorded in table 2. Values of α are greater than 2, which indicate that mode of fine particles exist. Fine particles included aerosol particles which are pollutant particles that can affect visibility as well as health and environment.

Calculations of visibility at wavelength 550nm using equation 7 are done and the results were recorded in table 3. Visibility values are between 10.52km and 52.58km. These visibility values are comparable to the values recorded in a polluted city like Mexico City (Eidels-Dubovoi, 2002) and Irbid city, Jordan (Hamasha, K. M. 2010). Since measurements were done in the city center of Tabuk. The city center site is impacted by local urban and regional aerosols. It is crowded with heavy traffic of all types of vehicles including heavy duty diesel buses and trucks. This study indicates that there are a lot of pollutant aerosols in the air that affect the visibility. Other sources of air pollution in the city are the industries, agriculture and traffic, as well as energy generations. During combustion processes and other production processes air pollutants are emitted. Some of these substances are not directly damaging to air quality, but will form harmful air pollutants by reactions with other substances that are present in air. Tabuk city has many Sources of air pollution besides the heavy traffic as (www.mic.gov.sa): the fumes rising from Tabuk cement factory, the industrial workshops, and many factories such as iron, chemical and agriculture factories.

The weather plays an important role in the formation and disappearance of air pollution. This is mainly influenced by wind and temperatures. Air pollutants can be transported by wind, causing a pollution to spread widely. Tabuk city is affected by regional aerosols because of it is close to Jordan and Siena, Egypt.

Conclusions

aerosol optical thickness (AOT) were obtained at the wavelength of 870 nm using handheld sun photometer and at the wavelengths of 550nm and 660nm using the MODIS satellite maps during 6-17 July, 2012 at Tabuk city center site. The calculations of the angstrom parameter α using the data of AOT for each day show values ranging between 2.21 and 6.39 which indicate that the atmosphere of Tabuk city has air pollutants in the range of fine particles. The average visibility attributed to aerosol at the City Center site dominated by urban scale and regional scale was ranging from 11km to 53km.

Acknowledgments

The authors acknowledge the financial support by grant number S-021-1433 from the Deanship of Scientific Research and Graduate Studies at Tabuk University, SA.
I would like also to thanks Dr. Patrick Arnott from the Physics Department at the University of Nevada/Reno for sending me a handheld sun photometer.

References

Brook, D. R., F. M. Mims III, T. Nguyen, and S. Bannasch, 1998, Characterization of LED-based sun photometers for use as GLOBE instruments. Proc. Third Annual GLOBE Conf. Snowmass, CO, GLOBE, 217-222.

Director General Administration of Environmental Health. Retrieved 27 November 2012 from http: www.mic.gov.sa.

Eck, T.F., B.N.Holben, J.S.Reid, O.Dubovik, A.Smirnov,N.T.O'Neill,I.Slutsker, and S.Kinne,1999, Wavelength dependence of the optical depth of biomass burning, urban and desert dust aerosol, J. Geophys. Res., 104,31 333-31 350.

Eidels-Dubovoi, S., (2002), Aerosol impacts on visible light extinction in the atmosphere of Mexico City, The science of total environment, 287, 213-220.

Hamasha, K. M., 2010, Visibility degradiation and light scattering/absorption due to aerosol particles in urban/suburban atmosphere of Irbid, Jordan, *JJP*, volume3, No.2, pp. 83-93.

Levy, R., Remer, L., Mattoo, S., Vermote, E., and Kaufman, Y., 2007, Second-generation algorithm for retrieving aerosol properties over land from MODIS spectral reflectance, J. Geophys. Res., 112(D13), D3211, doi:10.1029/2006JD007811.

Remer, L. A., Kleidman, R. G., Levy, R., Kaufman, Y., Tanre, D., Matto, S., Martins, G., Ichoko,C., Koren, I., Yu, H., and Holben, B. N., 2008, Global aerosol climatology from the MODIS sattalite sensors, J. Geophysics. Res., 113 (D14), D14S07,doi: 1029/2007JD009661.

Remer, L. A., Tanre, D., Kaufman, Y., Levy, R., and Matto, S., 2009, Algorithm for remote sensing of tropospheric aerosol from MODIS: collection 005, Rev. 2, 97 pp.

Vermote, E. F., Vibert, S., Kilcoyne, H., Hoyt, D., and Zhao, T., 2002, Suspended Matter. Visible/Infrard Imager/Radiometer Suite algorithm theoretical basis document. SBRS Document # Y2390, Raytheon Systems Company, Information Technology and Scientific Services, Maryland.

Wang, J. and Christopher, S. A., 2003: Intercomparison between satellite-derived aerosol optical thickness and $PM_{2.5}$ mass: Implications for air quality studies, Geophysics. Lett., 30(21), 2095, doi: 10.1029/2003GL018174.

Figure 1 map of Saudi Arabia shows the location of Tabuk city

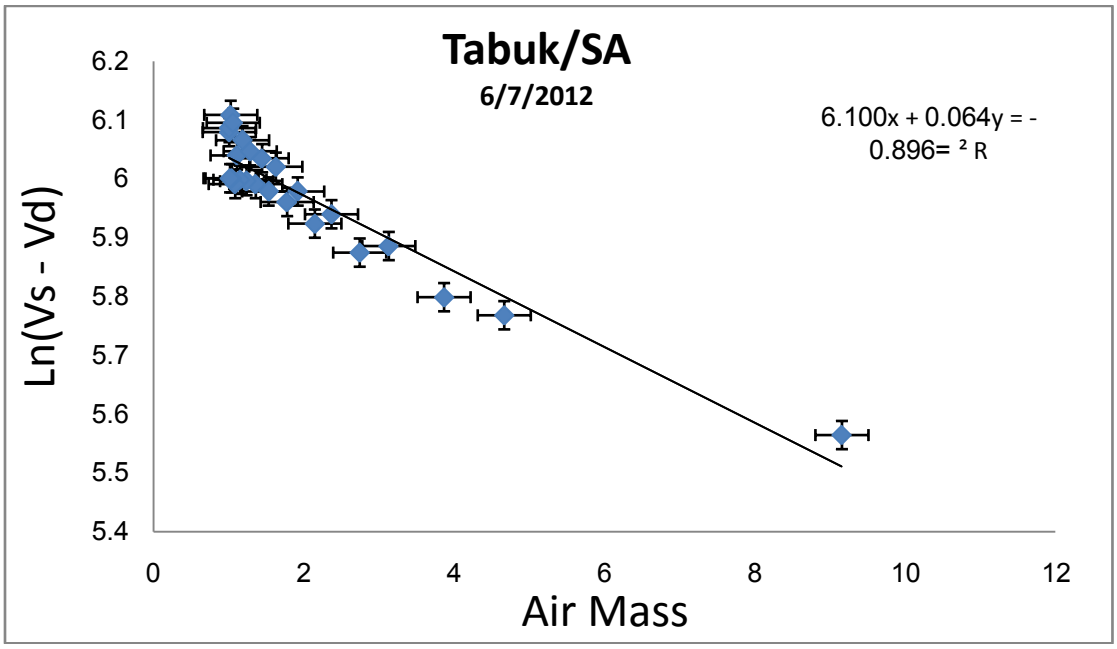

Figure 2. A linear correlation between air mass and natural logarithm of the difference of measurements between the sun signal and the dark signal. Measurements done using hand hold sun photometer at wavelength of 870 nm, during the day of 6th July 2012.

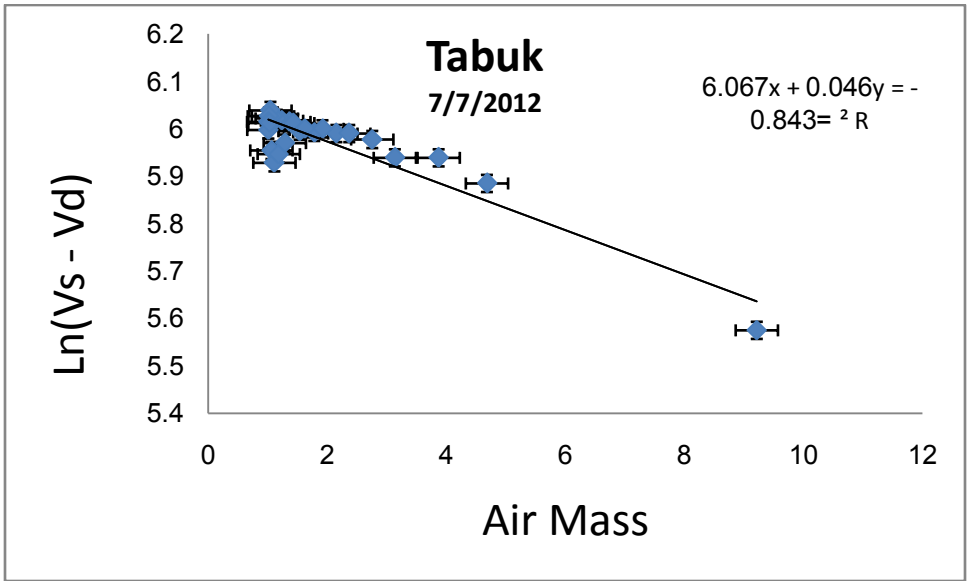

Figure 3. A linear correlation between air mass and natural logarithm of the difference of measurements between the sun signal and the dark signal. Measurements done using hand hold sun photometer at wavelength of 870 nm, during the day of 7th July 2012.

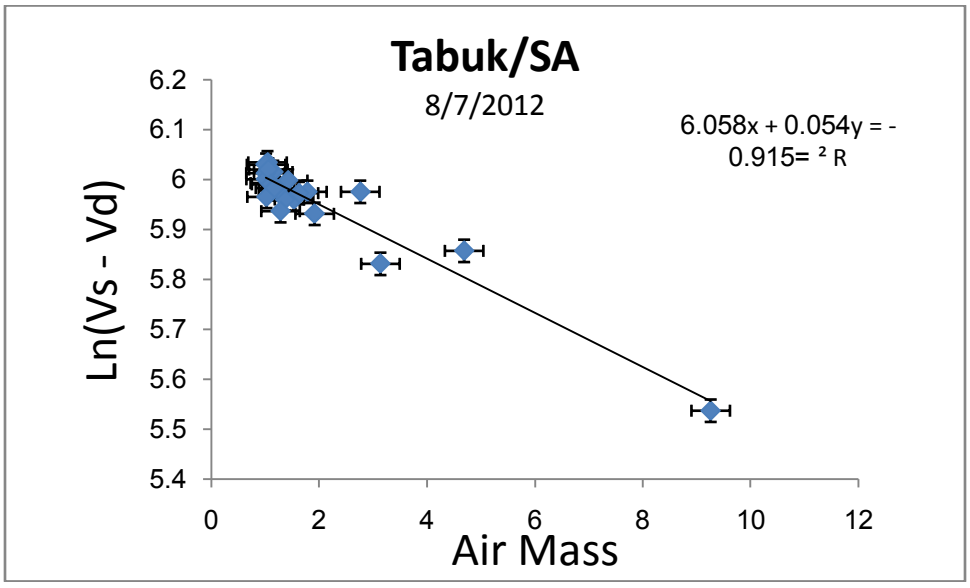

Figure 4. A linear correlation between air mass and natural logarithm of the difference of measurements between the sun signal and the dark signal. Measurements done using hand hold sun photometer at wavelength of 870 nm, during the day of 8th July 2012.

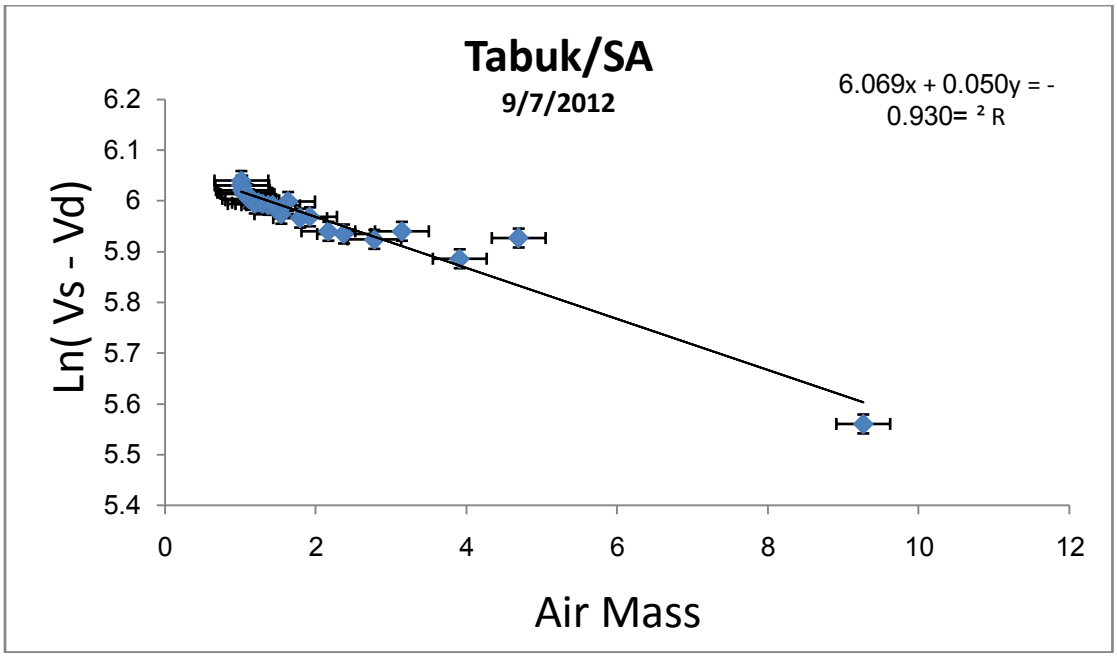

Figure 5. A linear correlation between air mass and natural logarithm of the difference of measurements between the sun signal and the dark signal. Measurements done using hand hold sun photometer at wavelength of 870 nm, during the day of 9th July 2012.

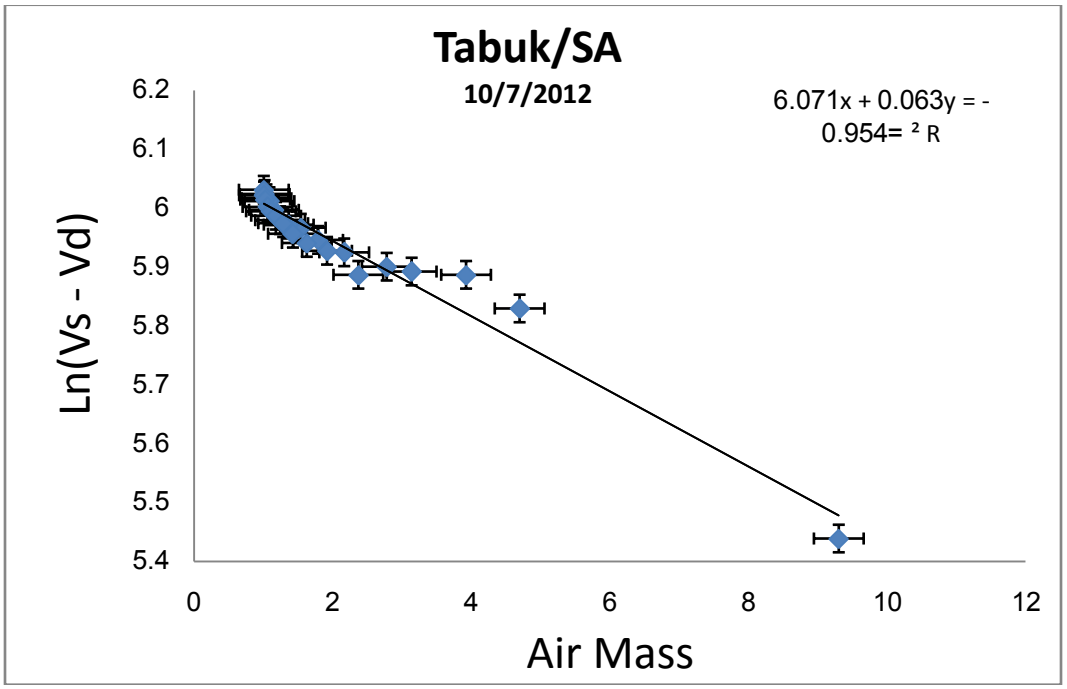

Figure 6. A linear correlation between air mass and natural logarithm of the difference of measurements between the sun signal and the dark signal. Measurements done using hand hold sun photometer at wavelength of 870 nm, during the day of 10th July 2012.

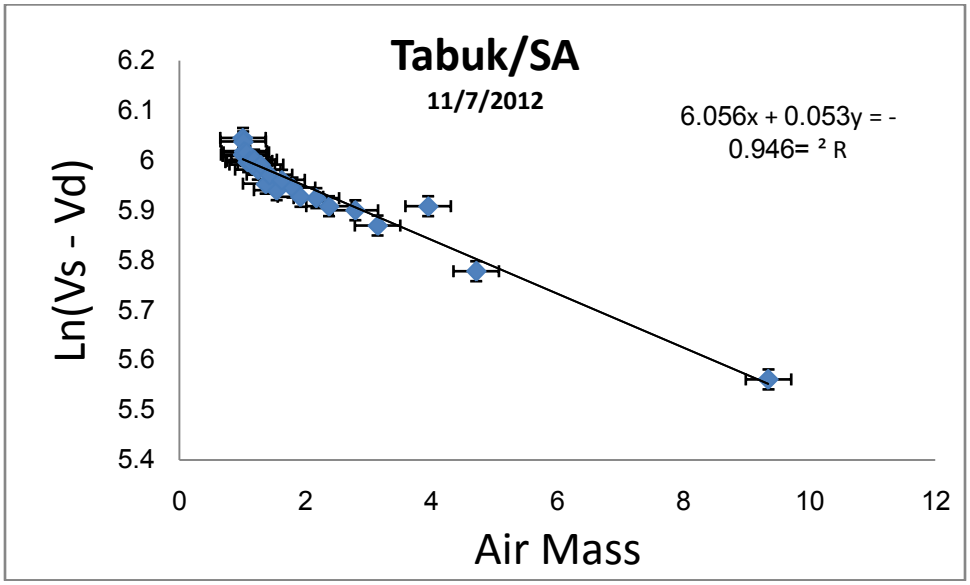

Figure 7. A linear correlation between air mass and natural logarithm of the difference of measurements between the sun signal and the dark signal. Measurements done using hand hold sun photometer at wavelength of 870 nm, during the day of 11th July 2012.

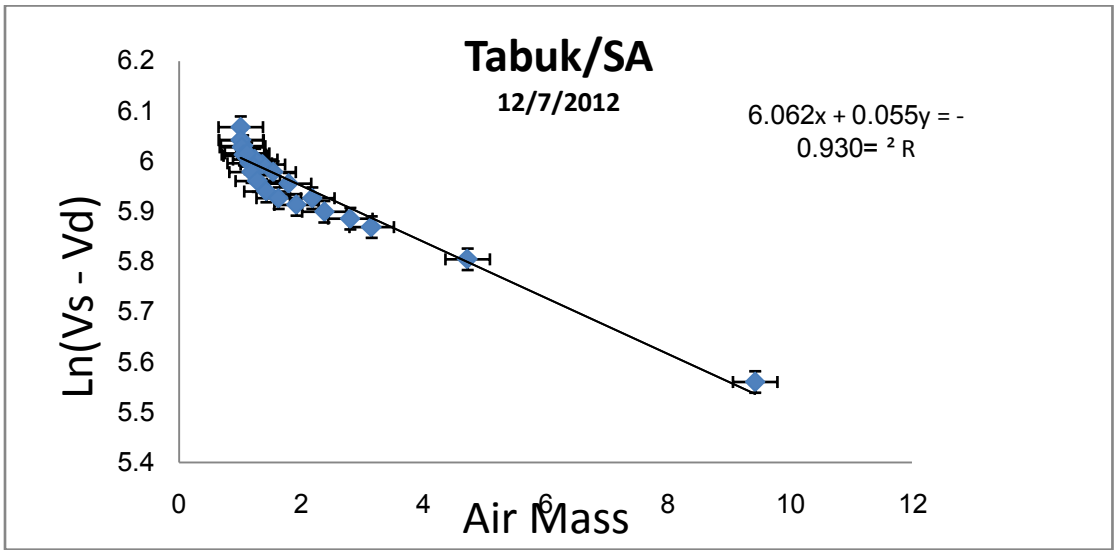

Figure 8. A linear correlation between air mass and natural logarithm of the difference of measurements between the sun signal and the dark signal. Measurements done using hand hold sun photometer at wavelength of 870 nm, during the day of 12th July 2012.

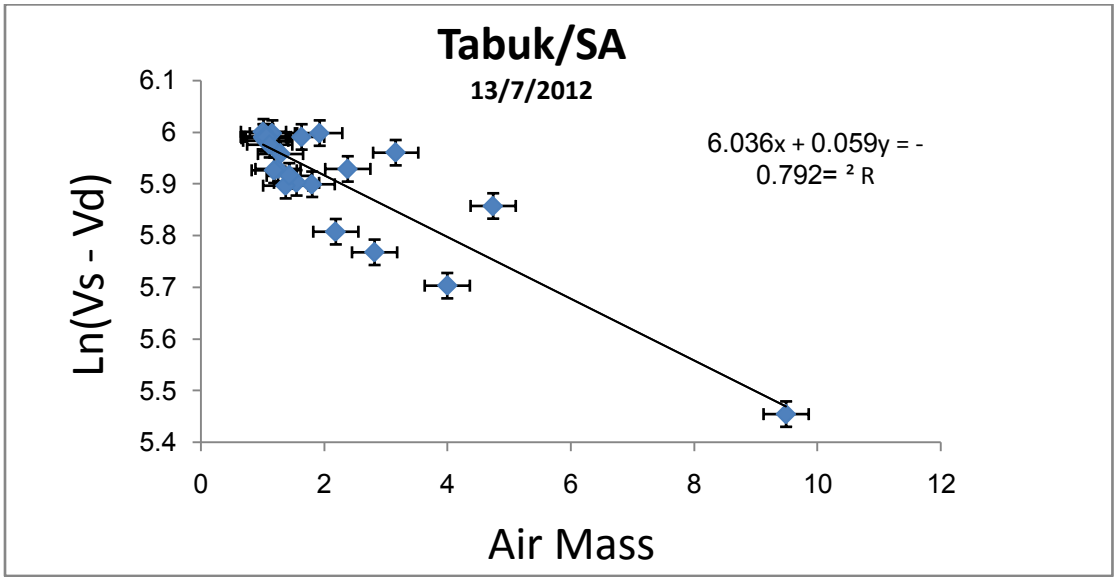

Figure 9. A linear correlation between air mass and natural logarithm of the difference of measurements between the sun signal and the dark signal. Measurements done using hand hold sun photometer at wavelength of 870 nm, during the day of 13th July 2012.

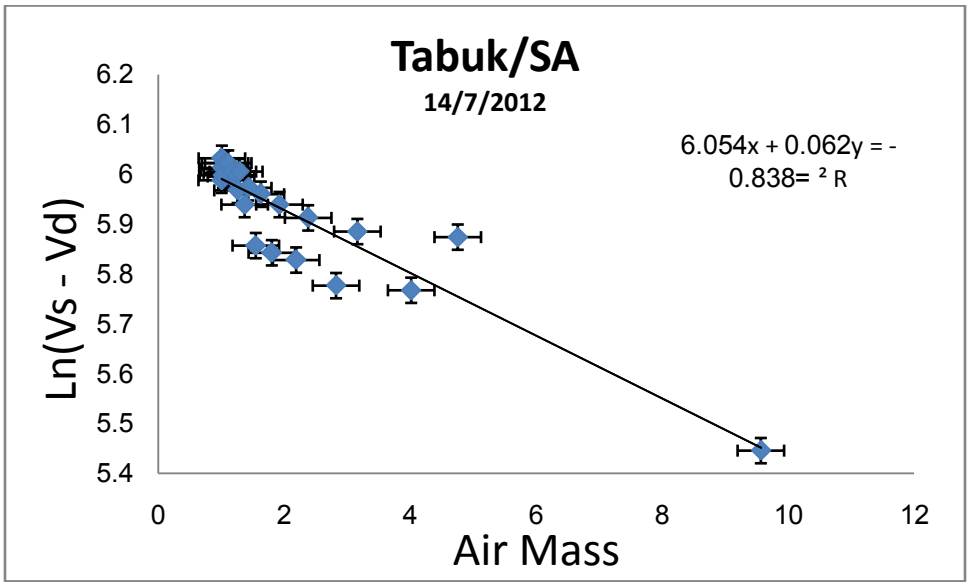

Figure 10. A linear correlation between air mass and natural logarithm of the difference of measurements between the sun signal and the dark signal. Measurements done using hand hold sun photometer at wavelength of 870 nm, during the day of 14th July 2012.

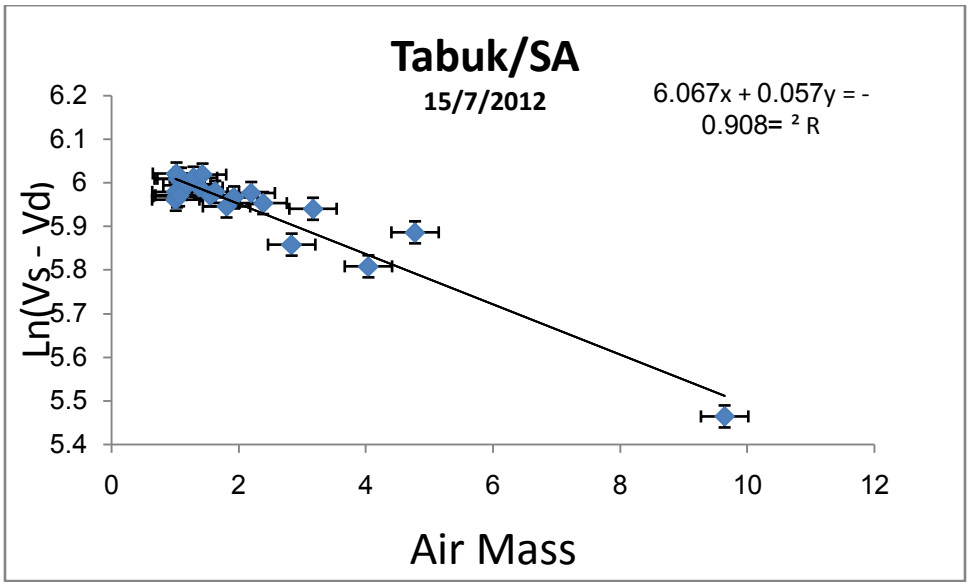

Figure 11 A linear correlation between air mass and natural logarithm of the difference of measurements between the sun signal and the dark signal. Measurements done using hand hold sun photometer at wavelength of 870 nm, during the day of 15th July 2012.

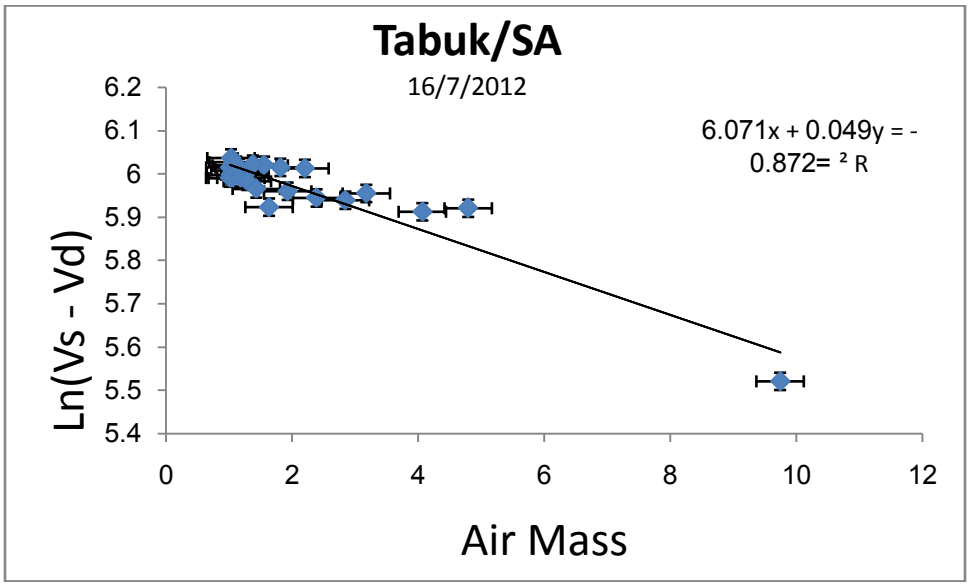

Figure 12. A linear correlation between air mass and natural logarithm of the difference of measurements between the sun signal and the dark signal. Measurements done using hand hold sun photometer at wavelength of 870 nm, during the day of 16th July 2012.

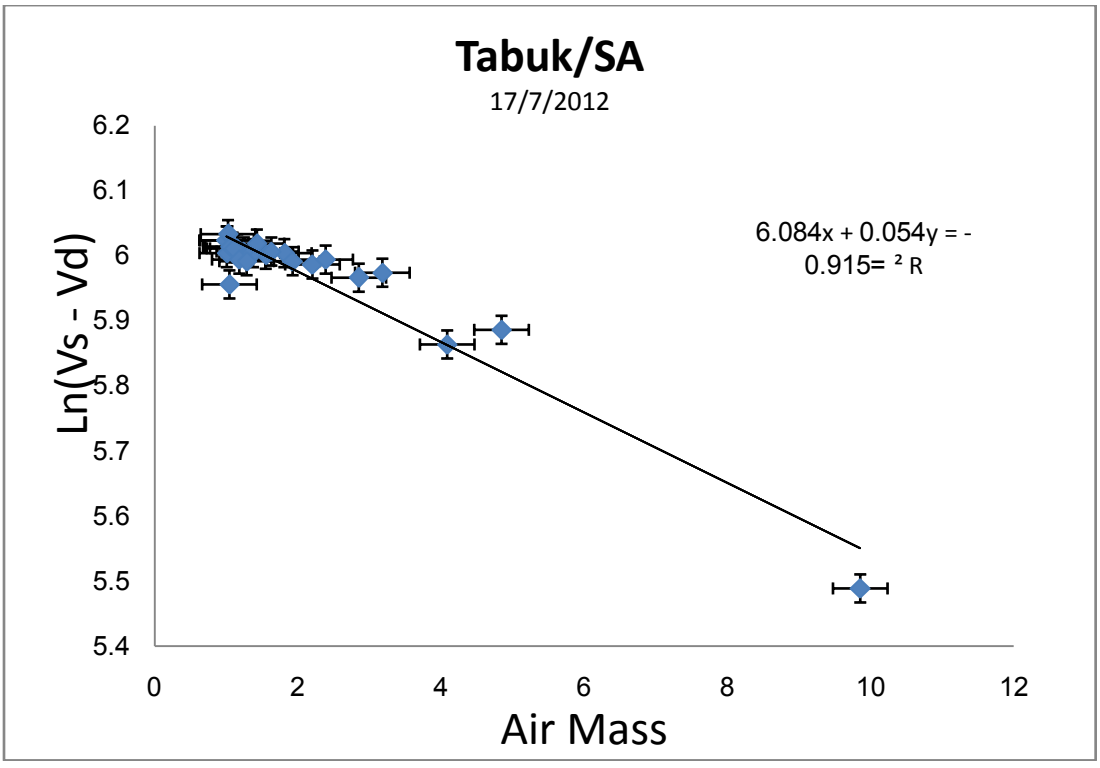

Figure13. A linear correlation between air mass and natural logarithm of the difference of measurements between the sun signal and the dark signal. Measurements done using hand hold sun photometer at wavelength of 870 nm, during the day of 17th July 2012.

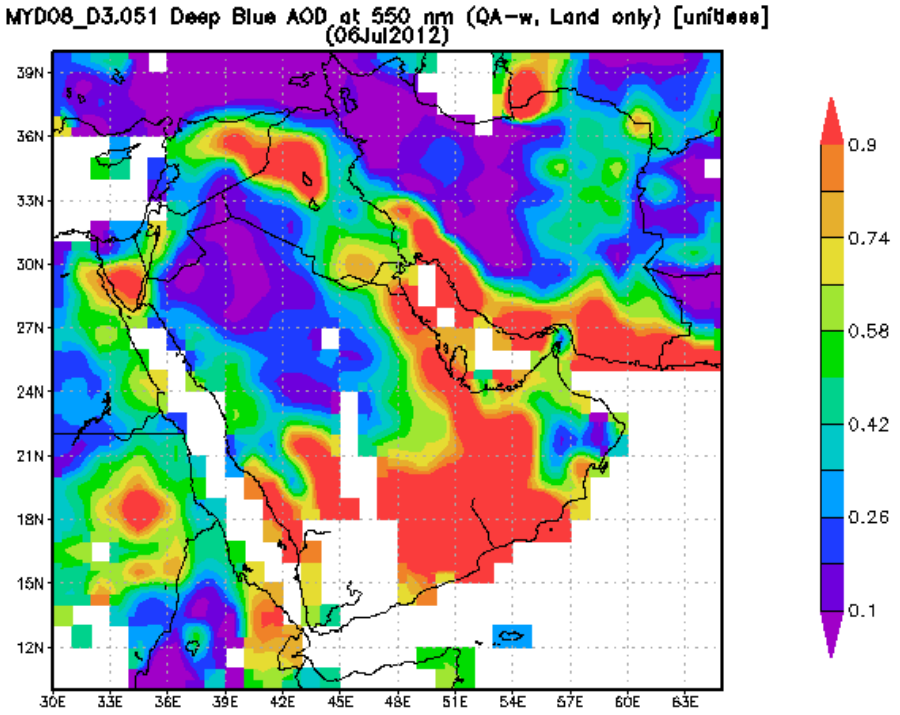

Figure 14. Satellite map for AOT on 6 July 2012 at the wavelength of 550 nm

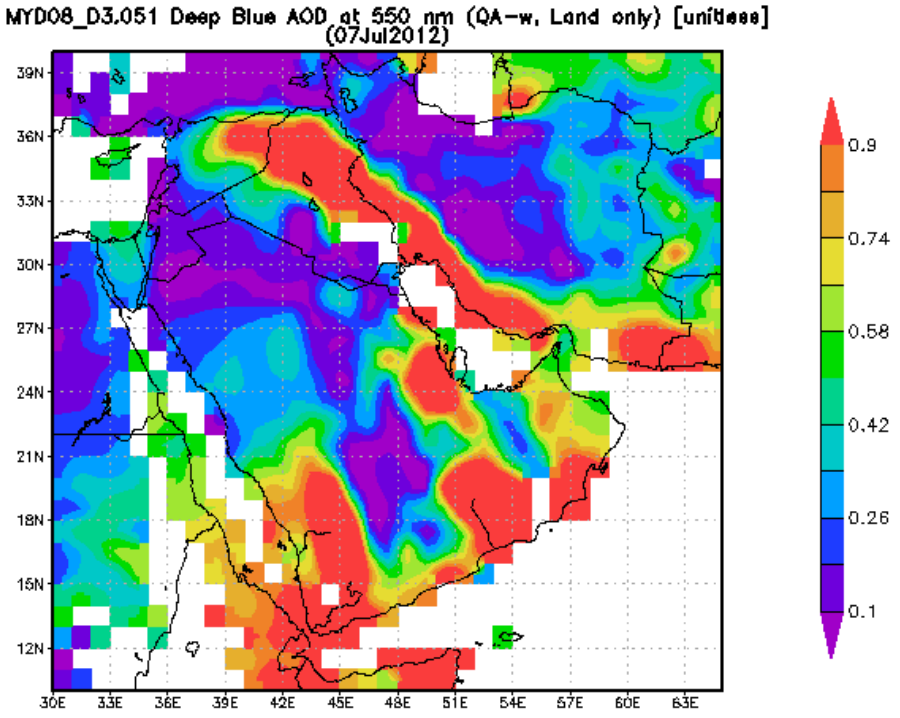

Figure 15. Satellite map for AOT on 7 July 2012 at the wavelength of 550 nm

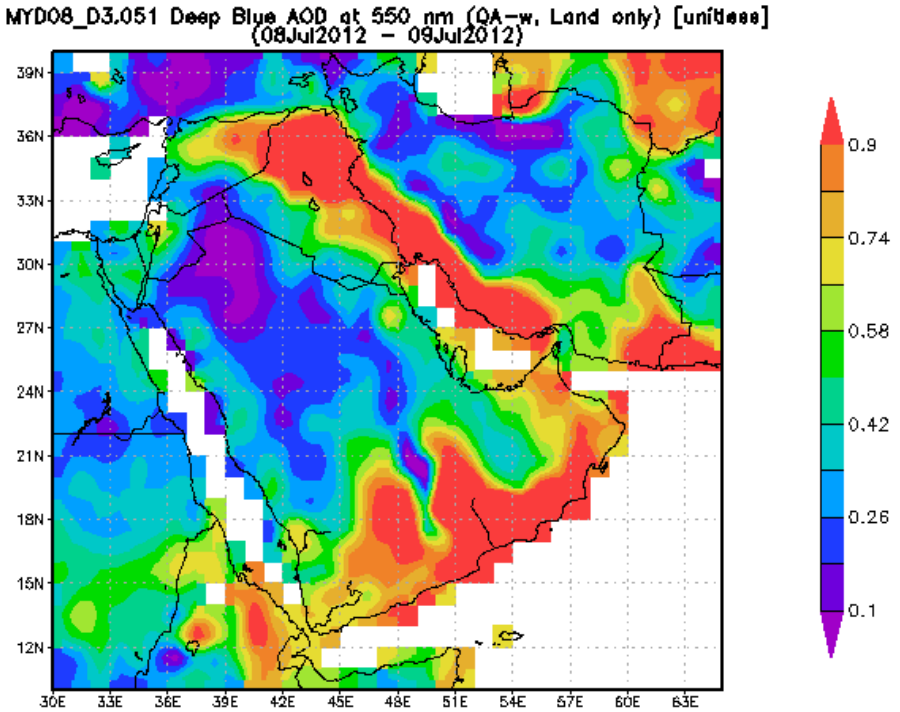

Figure 16. Satellite map for AOT on 8 July 2012 at the wavelength of 550 nm

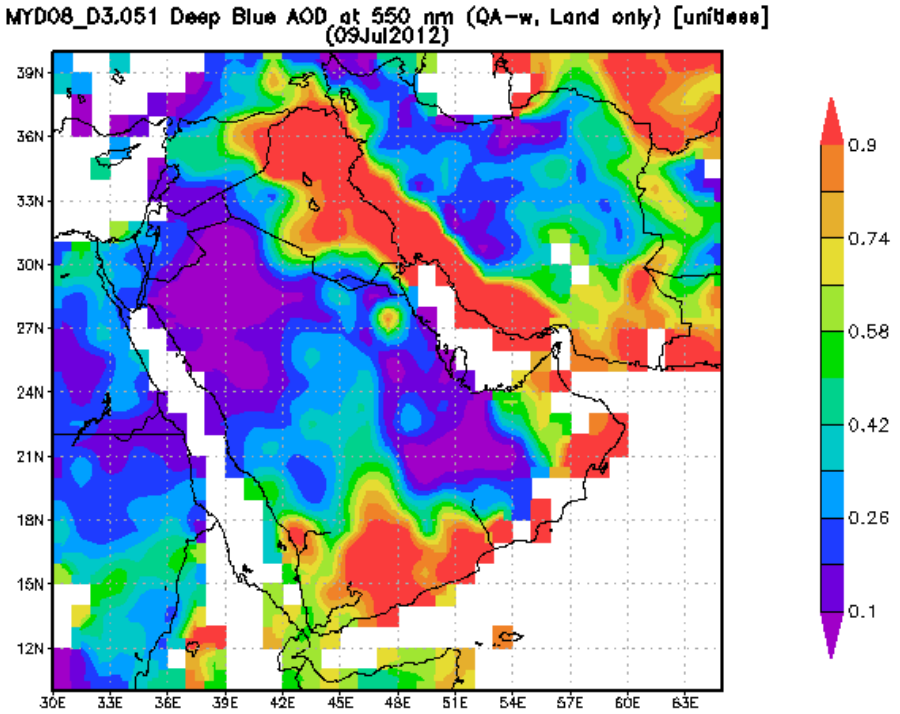

Figure 17. Satellite map for AOT on 9 July 2012 at the wavelength of 550 nm

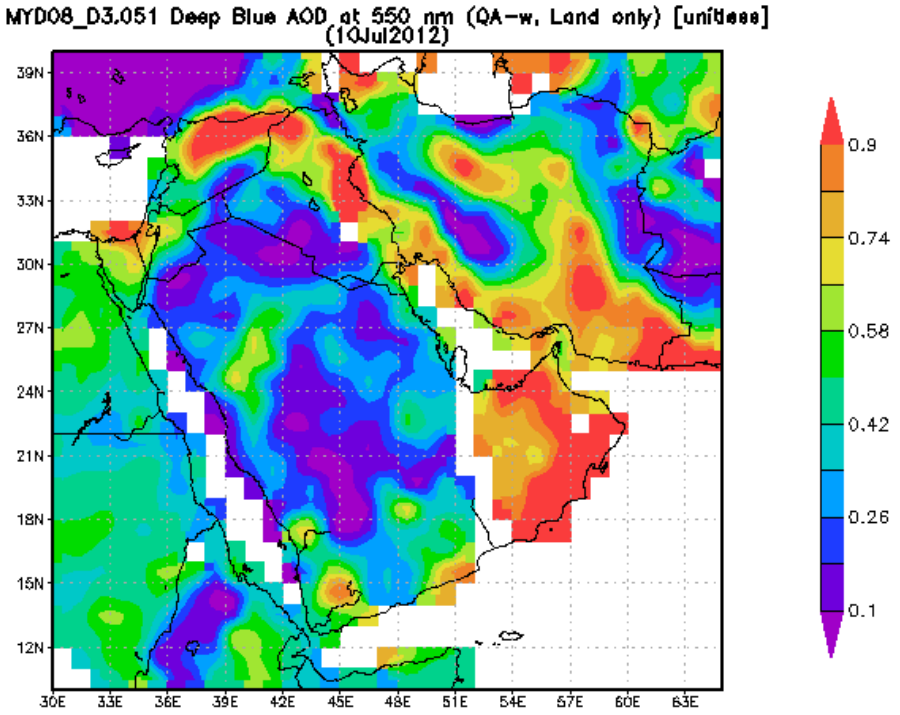

Figure 18. Satellite map for AOT on 10 July 2012 at the wavelength of 550 nm.

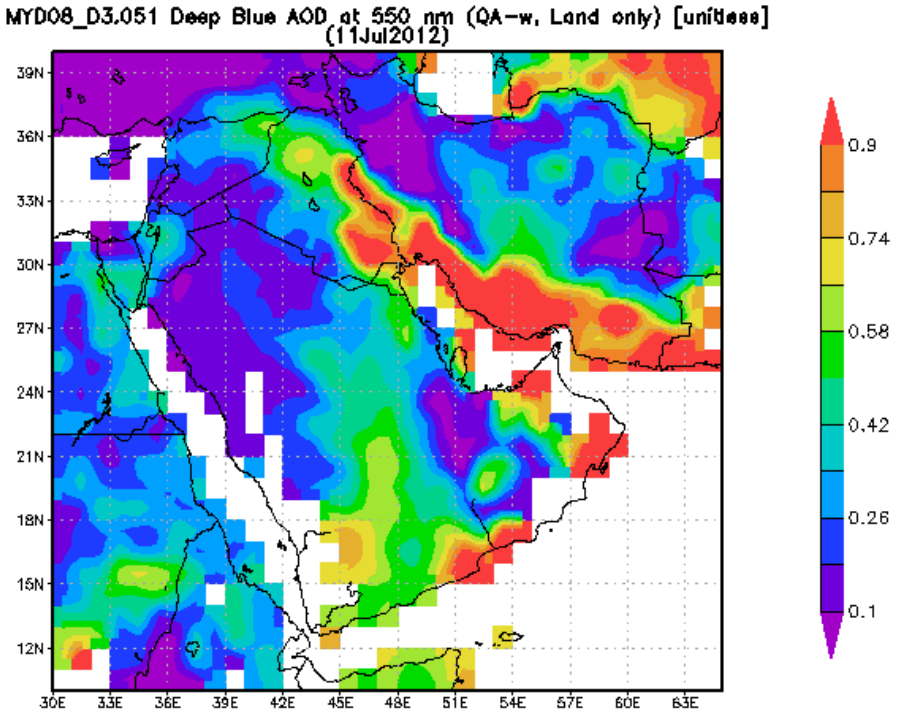

Figure 19. Satellite map for AOT on 11 July 2012 at the wavelength of 550 nm.

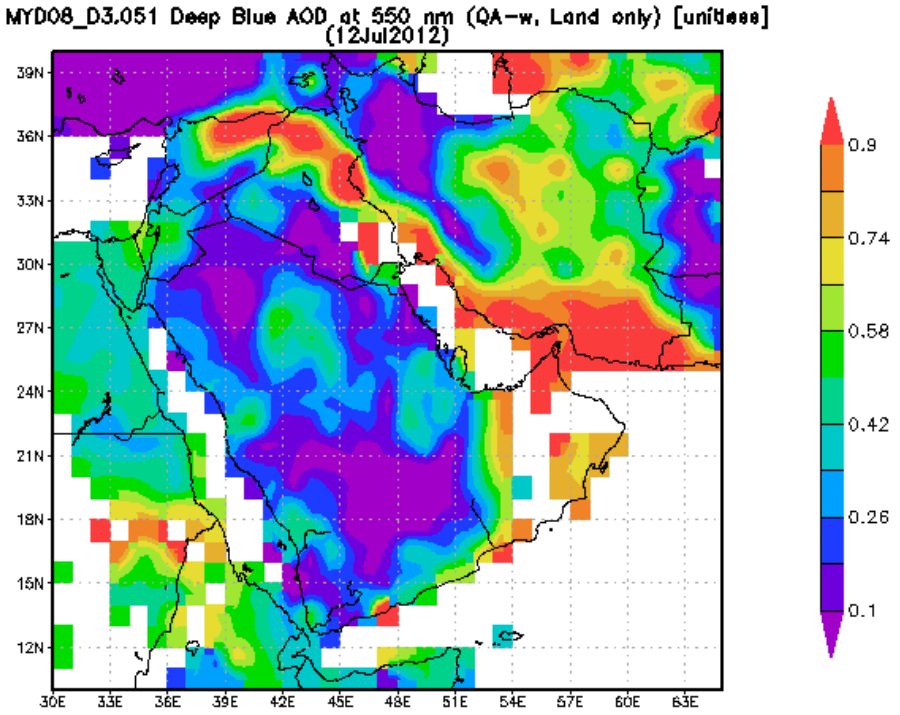

Figure 20. Satellite map for AOT on 12 July 2012 at the wavelength of 550 nm.

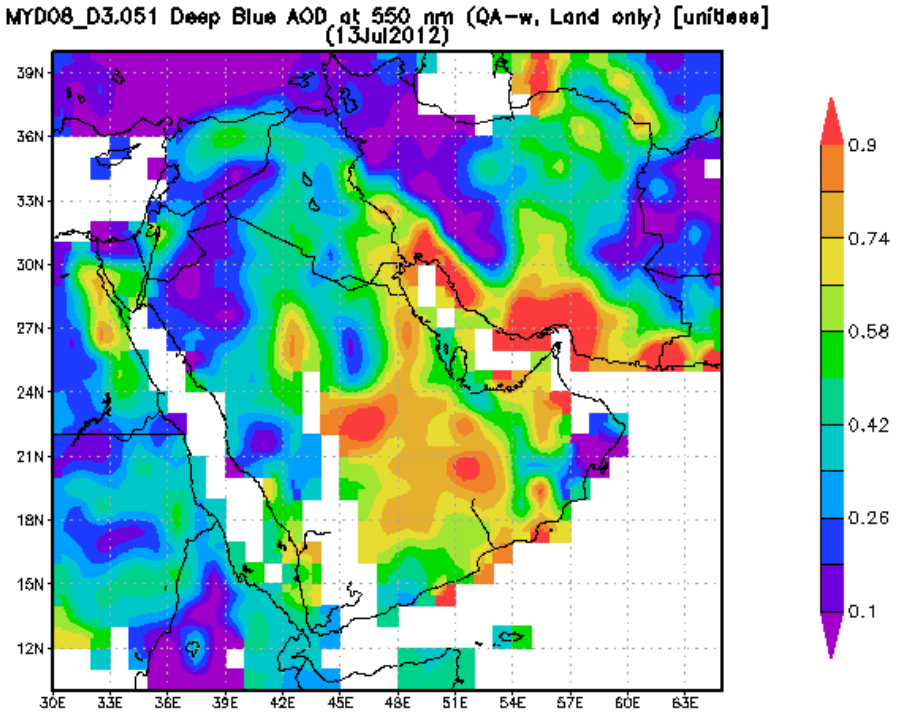

Figure 21. Satellite map for AOT on 13 July 2012 at the wavelength of 550 nm.

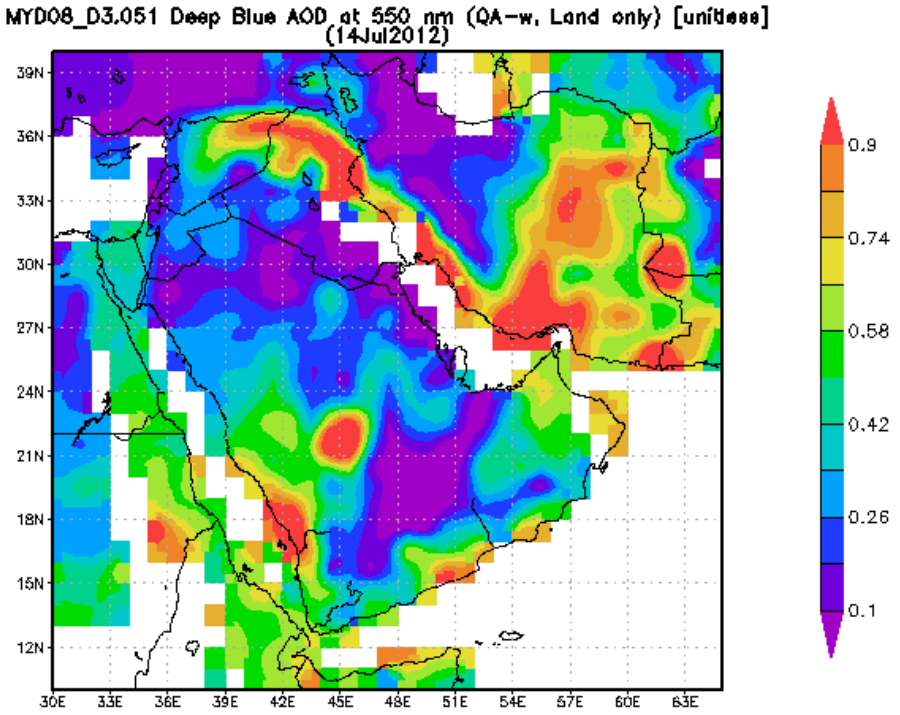

Figure 22. Satellite map for AOT on 14 July 2012 at the wavelength of 550 nm.

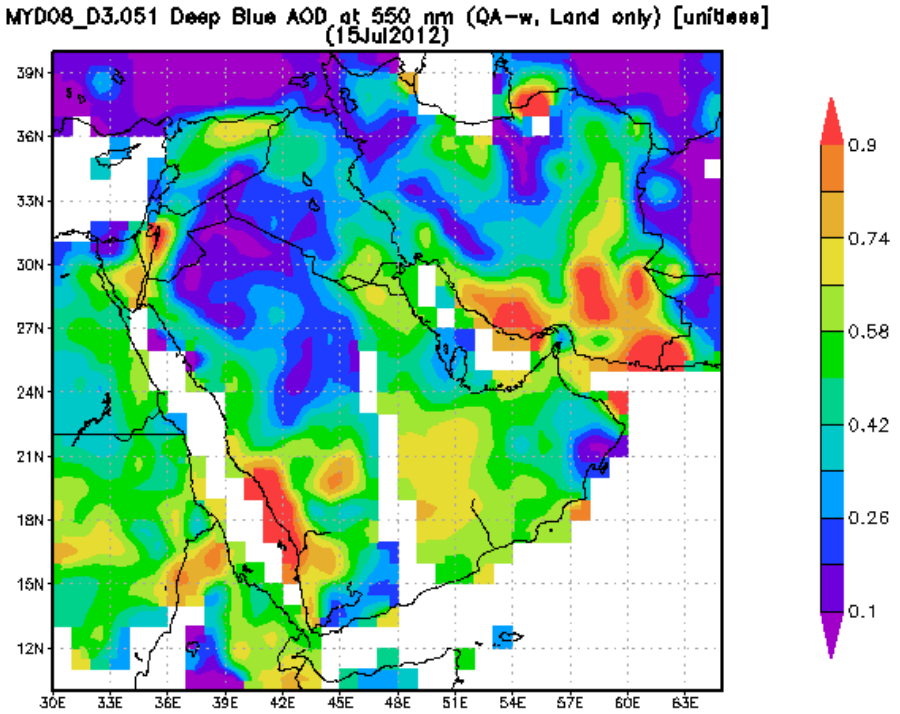

Figure 23. Satellite map for AOT on 15 July 2012 at the wavelength of 550 nm.

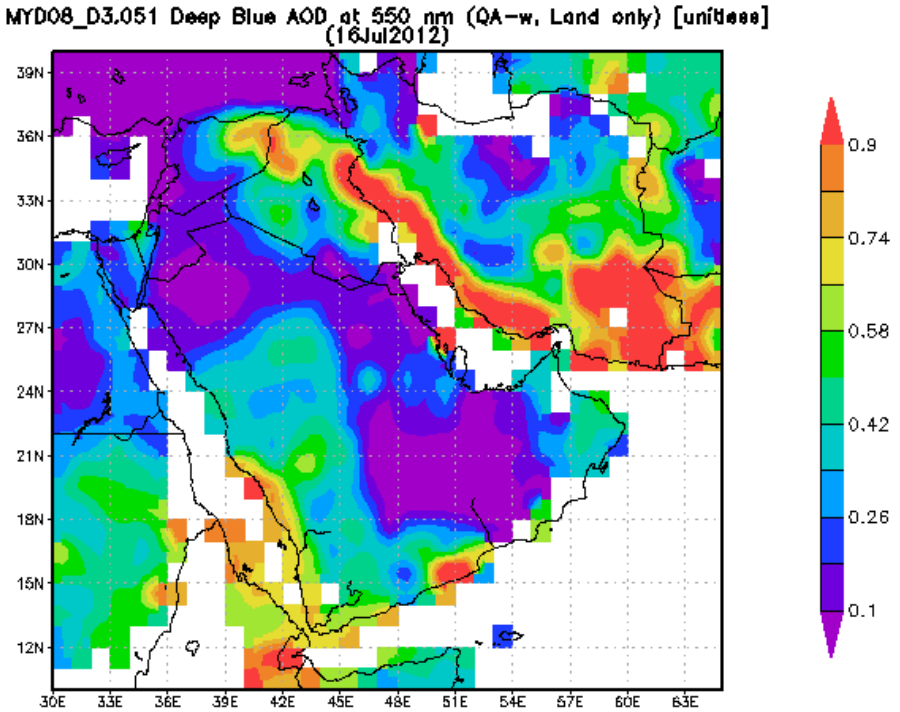

Figure 24. Satellite map for AOT on 16 July 2012 at the wavelength of 550 nm.

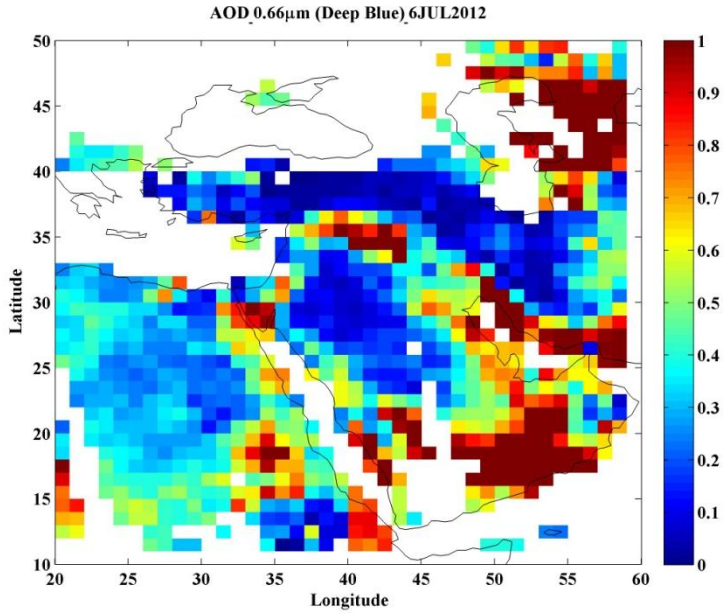

Figure 25. Satellite map for AOT on 6 July 2012 at the wavelength of 660 nm.

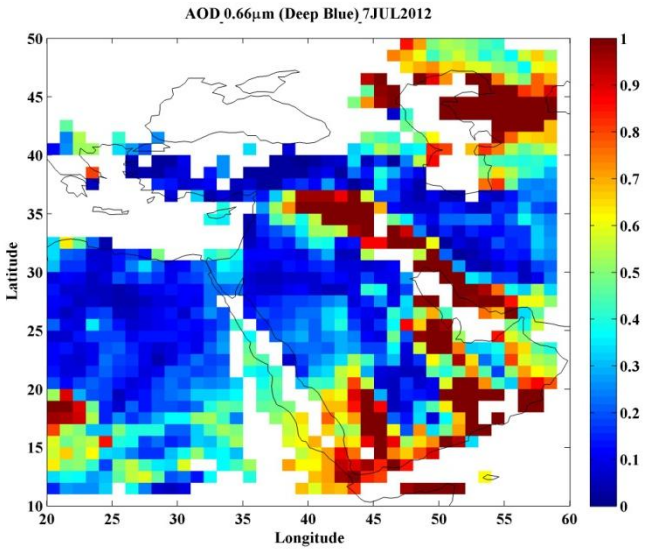

Figure 26. Satellite map for AOT on 6 July 2012 at the wavelength of 660 nm.

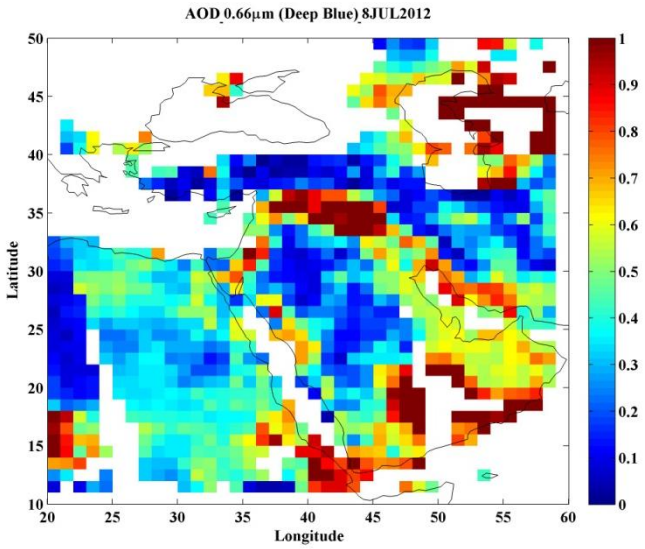

Figure 27. Satellite map for AOT on 8 July 2012 at the wavelength of 660 nm.

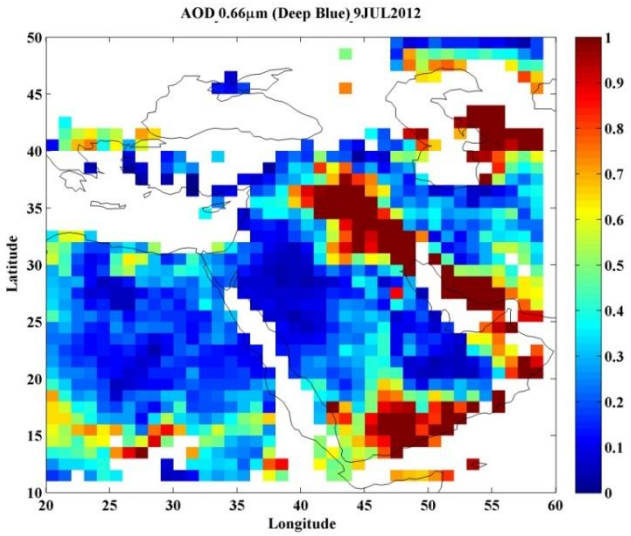

Figure 28. Satellite map for AOT on 9 July 2012 at the wavelength of 660 nm.

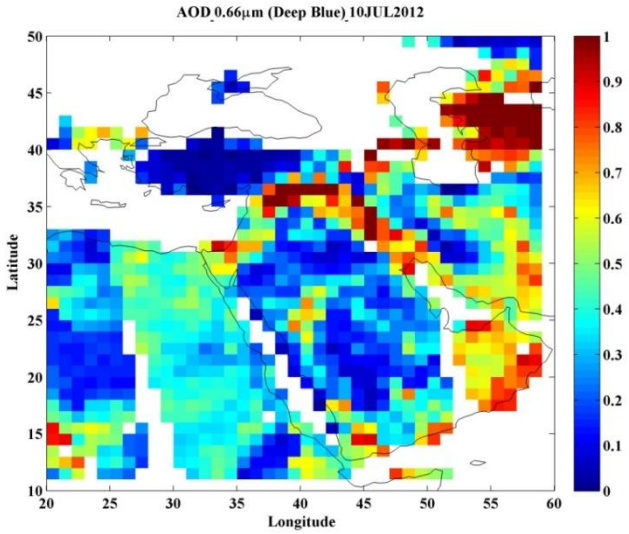

Figure 29. Satellite map for AOT on 10 July 2012 at the wavelength of 660 nm.

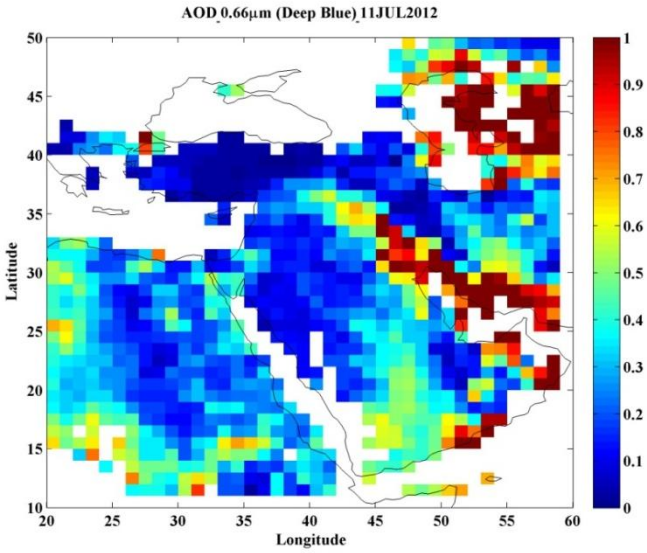

Figure 30. Satellite map for AOT on 11 July 2012 at the wavelength of 660 nm.

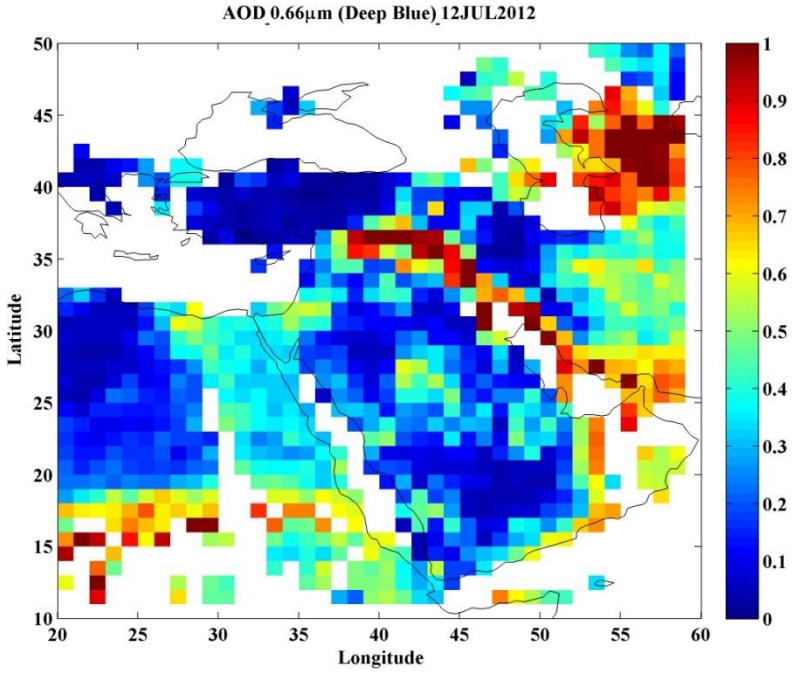

Figure 31. Satellite map for AOT on 12 July 2012 at the wavelength of 660 nm.

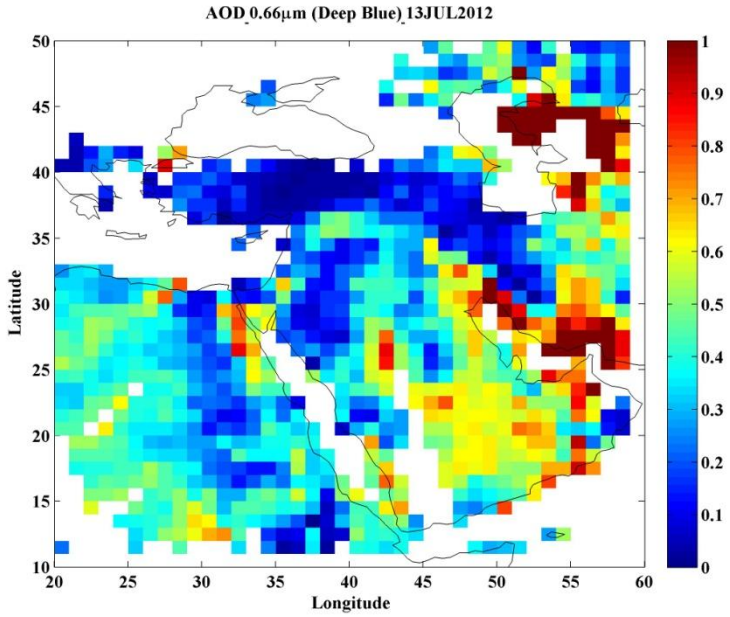

Figure 32. Satellite map for AOT on 13 July 2012 at the wavelength of 660 nm.

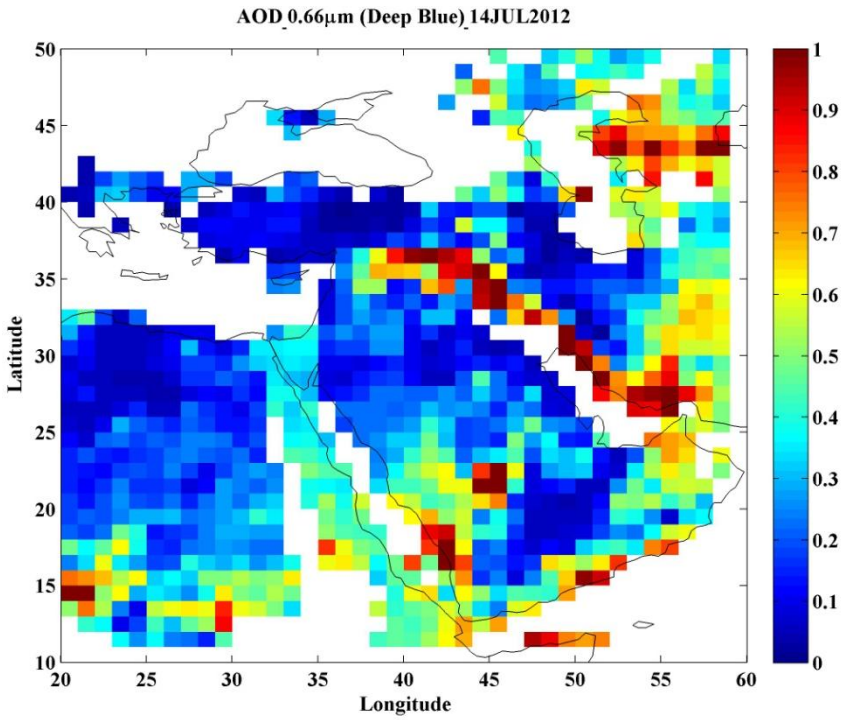

Figure 33. Satellite map for AOT on 14 July 2012 at the wavelength of 660 nm.

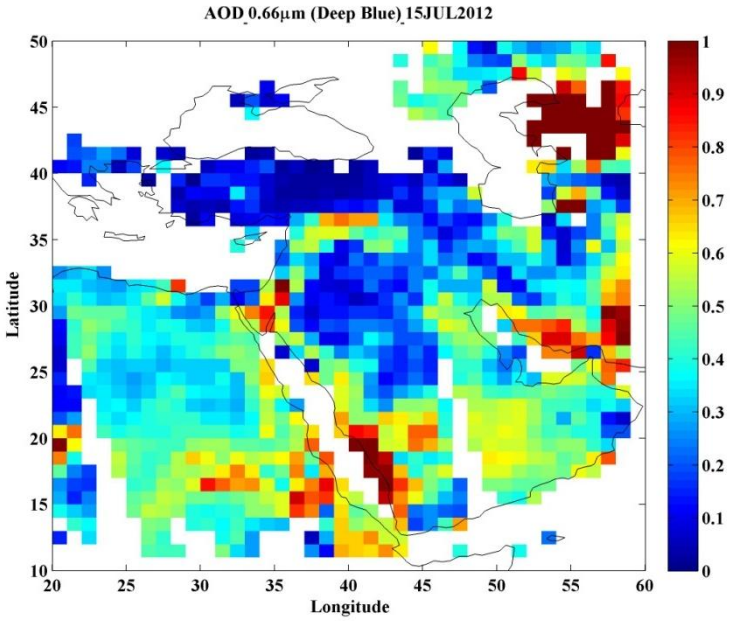

Figure 34. Satellite map for AOT on 15 July 2012 at the wavelength of 660 nm.

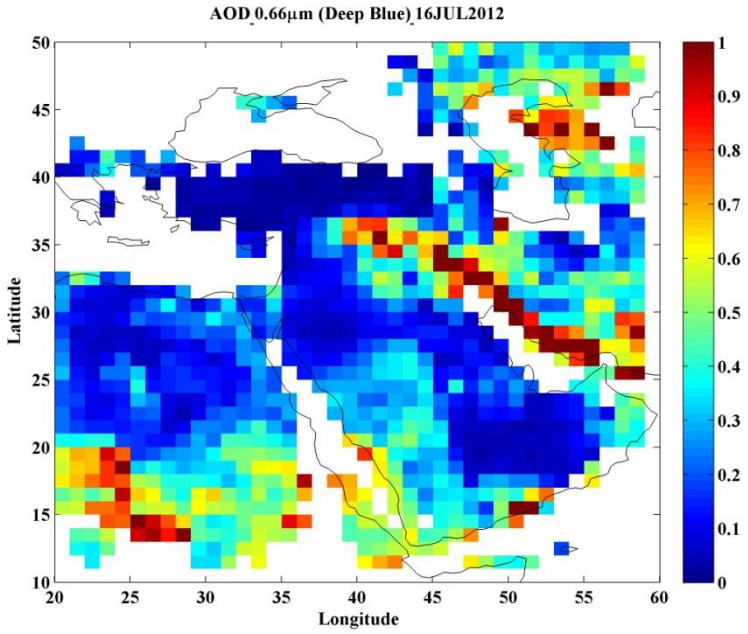

Figure 35. Satellite map for AOT on 16 July 2012 at the wavelength of 660 nm.

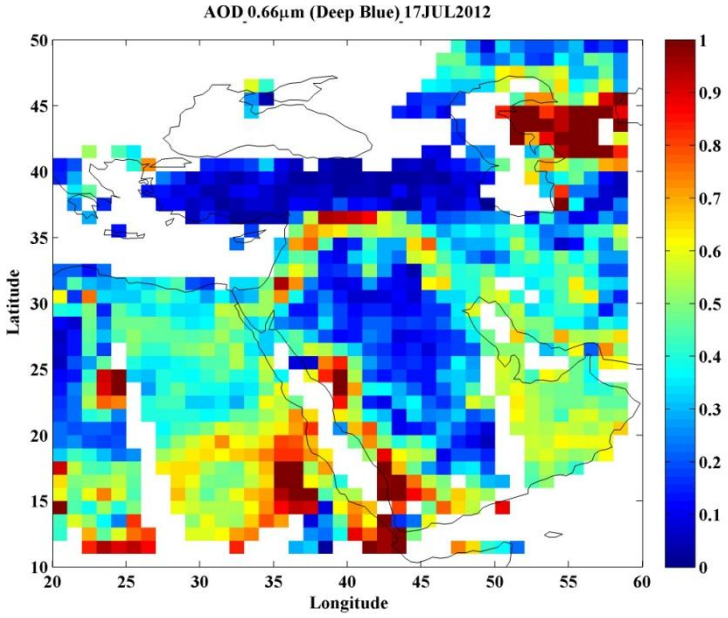

Figure 36. Satellite map for AOT on 17 July 2012 at the wavelength of 660 nm.

Table 1: Data of AOT in Tabuk city for the period 6 – 17 July 2012 at the wavelengths 550nm, 660nm and 870nm.

AOT(550nm)	AOT(660nm)	AOT(870nm)	date
0.18	0.3	0.065	06/07/12
0.18	0.15	0.047	07/07/12
0.18	0.35	0.054	08/07/12
0.16	0.1	0.05	09/07/12
0.22	0.2	0.064	10/07/12
0.2	0.2	0.054	11/07/12
0.26	0.2	0.056	12/07/12
0.18	0.25	0.06	13/07/12
0.1	0.15	0.063	14/07/12
0.34	0.6	0.058	15/07/12
0.18	0.2	0.05	16/07/12
0.34	0.25	0.054	17/07/12

Table 2: Exponent parameters calculated from the three wavelengths using the least squares fit.

$R^{\wedge 2}$	β	α	date
0.75	-2.99	3.25	06/07/12
0.69	-3.28	3.18	07/07/12
0.76	-3.23	3.45	08/07/12
0.79	-3.25	2.97	09/07/12
0.77	-3.00	3.08	10/07/12
0.69	-3.11	2.85	11/07/12
0.72	-3.15	3.61	12/07/12
0.78	-3.09	3.41	13/07/12
0.69	-2.92	2.21	14/07/12
0.76	-3.23	4.84	15/07/12
0.88	-3.26	2.65	16/07/12
0.99	-3.78	6.39	17/07/12

Table 3: Visibility values calculated using the AOT data at 550nm wavelength

V(km)	date
22.54	06/07/12
41.52	07/07/12
20.23	08/07/12
41.52	09/07/12
25.45	10/07/12
34.29	11/07/12
22.54	12/07/12
22.54	13/07/12
52.58	14/07/12
10.52	15/07/12
41.52	16/07/12